Process intensification of the catalytic hydrogenation of squalene using a Pd/CNT catalyst combining nanoparticles and single atoms in a continuous flow reactor

Laurent Vanoye, Boris Guicheret, Camila Rivera-Cárcamo, Ruben Castro Contreras, Claude de Bellefon, Valérie Meille, Philippe Serp, Régis Philippe, Alain Favre-Réguillon

Process intensification of the catalytic hydrogenation of squalene using a Pd/CNT catalyst combining nanoparticles and single atoms in a continuous flow reactor.

Laurent Vanoye [a], Boris Guicheret [a], Camila Rivera-Cárcamo [b], Ruben Castro Contreras [b], Claude de Bellefon [a], Valérie Meille [a], Philippe Serp [b], Régis Philippe [a,*], Alain Favre-Réguillon [a,c,*]

[a] *Université de Lyon, Catalyse, Polymérisation, Procédés & Matériaux (CP2M), UMR 5128 CNRS – CPE Lyon – Université Claude Bernard Lyon 1, F-69100 Villeurbanne, France.*

[b] *Université de Toulouse, ENSIACET, LCC CNRS-UPR 8241, F-31030 Toulouse, France.*

[c] *Conservatoire National des Arts et Métiers, EPN7-CG, F-75003 Paris, France.*

Abstract

A process intensification study for the full hydrogenation of bio-derived platform molecule squalene (SQE) into squalane (SQA), using commercial heterogeneous Pd catalysts and Pd supported on carbon nanotubes (CNT) is reported. Pd/CNT shows a substantial improvement of the catalytic activity for the total hydrogenation of SQE into SQA thanks to cooperativities between Pd nanoparticles and single atoms simultaneously present on the CNT. However, the stirred reactor's productivity, scalability, and operability are limited by the exothermicity of the reaction ($\Delta_r H$= - 765 kJ.mol^{-1}). The implementation of the Pd/CNT catalyst in flow was then studied after coating this catalyst on metallic open cell foams. Using the foam-based milli-reactor's characteristics, including high mass and heat transfer rates and safety, fully reduced SQA (> 99 %) was obtained at 180 °C and 30 bar of H_2 for a contact time of 1.45 min with a space-time yield of 68 $mol_{SQA}.mol_{Pd}^{-1}.min^{-1}$. Finally, a scale-up strategy (7 fold) was successfully attempted in a commercially available pilot-scale reactor

that meets further seamless scale-up requirements. A production capacity of 2 kg per day using a commercial intensified reactor with a reacting volume of 43.2 mL was obtained under mild conditions (120°C and 30 bar of H_2).

Keywords: squalene · palladium · catalytic hydrogenation · carbon nanotube support · structured reactors · seamless scale-up.

* Corresponding authors at: *Université de Lyon, Catalyse, Polymérisation, Procédés & Matériaux (CP2M), UMR 5128 CNRS – CPE Lyon – Université Claude Bernard Lyon 1, F-69100 Villeurbanne, France* (R. Philippe and A. Favre-Réguillon).

E-mail addresses: regis.philippe@lgpc.cpe.fr (R. Philippe), afr@lgpc.cpe.fr (A. Favre-Réguillon).

1. Introduction

Squalene (SQE) is a linear triterpene (Figure 1) present in the cells of all living organisms and is a precursor for the synthesis of secondary metabolites such as sterols, hormones, or vitamins [1]. In 1916, M. Tsujimoto correctly identified its formula as $C_{30}H_{50}$ and named it squalene, referring to the fact that it was isolated from the liver oils of deep-sea sharks (*squalus spp.*) [2]. At present, SQE is used extensively in pharmaceuticals, food supplements, and cosmetics due to its multiple functions. The global SQE market size was higher than USD 110 million in 2016 and is expected to witness significant growth over the following years [3].

SQE demand has been mainly covered by extracting the deep-sea shark's liver oil for almost a century. However, due to sharks' slow growth, long reproductive cycles, and concomitant over-fishing, leading cosmetic companies have stopped using SQE from the marine source. Hence, new sources from plants [4, 5], biorefinery [6], or biotechnology are becoming increasingly important [1, 7-9], and SQE is now an interesting bio-derived platform molecule [10, 11].

SQE is a relatively stable molecule in the absence of oxygen [12]. In the presence of oxygen, SQE exerts a weak antioxidant activity due to competitive oxidation phenomena, leading to squalene oxidation products (SOPs, *i.e.* epoxides and alcohols, as well as scission products from the latter) [12]. These SOPs have a pro-oxidant activity that mitigates the global antioxidant activity. In order to increase stability, SQE could be fully hydrogenated to squalane (SQA) (Figure 1). This reduction was reported by M. Tsujimoto using Pt oxide catalyst (0.02 M in Et_2O, 1 atm H_2, r.t.) [2]. However, SQA had no practical use until 1950, when the French firm Laserson reduced SQE neat using a copper-chromite catalyst and marketed it under the trade name Cosbiol (perhydrosqualene) for cosmetic applications [13]. In particular, SQA was found non-comedogenic, unlike SQE, and behaves as a transparent, colorless, odorless, stable, and non-irritant emollient substance [14]. SQA, because of the high boiling point, inertness, low viscosity, and high gas solubility is also an attractive apolar

solvent used as a reaction medium for catalytic tests [15, 16] or for the synthesis of quantum dots [17], for example.

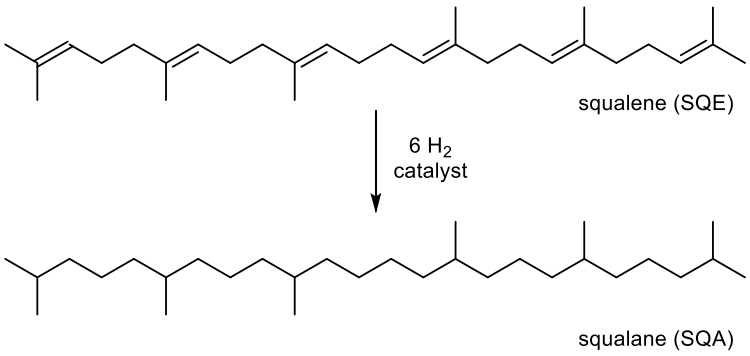

Figure 1. Full hydrogenation of squalene (SQE) into squalane (SQA) (See section 2.4 Analytical monitoring of the reaction progress for details).

The hydrogenation of SQE into SQA was mainly studied in a batch reactor under harsh conditions and high loading of Ni-based catalyst. The high metal loading and harsh conditions could be explained by the presence of impurities (wax, esters, …) that originated from the raw materials [18], *i.e.* originally sharks liver oil or currently from vegetable sources. However, this conventional reduction method produced by-product(s) with lousy smell(s) [19]. The by-product(s) structure is unknown but probably derived from bond migration induced by Ni catalyst and harsh conditions [20]. Consequently, product purification was necessary to obtain high-quality SQA, which raised the overall production costs. Furthermore, under those conditions, Ni leaching could be expected. Thus post purifications are required to decrease the concentration of toxic nickel compounds (Ni^{2+} and Ni^{0}) to the maximum acceptable levels in the cosmetic product (0.2 ppm) [21].

Recently, biotechnology processes were developed to produce microbial-derived SQE with less impurity and renew the interest in reducing the latter [10, 11]. Milder reaction conditions may be used to reduce SQE of the finest quality. In particular, M. Pagliaro *et al.* have studied the reduction of SQE (98 % purity) using encapsulated Pd nanoparticles within mesoporous organosilica (Siliacat® Pd). With this catalyst, a high yield (> 99.5 %) of SQA could be obtained under mild

conditions (*i.e.* 1 atm H_2 at 50 °C and in 4 h using 0.5 mol % of Pd in EtOH 0.33 M) [18]. The reduction of diluted SQE in a continuous reactor using innovative 3D printed catalytic supports was also recently described [22].

In this paper, the reduction of SQE into SQA was explored using a new and highly active Pd catalyst supported on carbon nanotubes under mild conditions and compared to commercially available catalysts. Batch stirred tank to intensified continuous reactor transposition has also been investigated.

2. Experimental section

2.1. Solvents, SQE and SQA

Analytical grade heptane and EtOH were purchased from Aldrich or Acros and used as received. SQE (≥ 98 %) was purchased from Aldrich and used as received. SQE was stored under refrigeration (2-8 °C) and protected from light. High purity SQA was produced by reducing SQE using Pd/Al_2O_3 under standard conditions (0.33M, 120 °C, 20 bar H_2). After completion of the reaction, the reaction mixture was filtrated over Celite. The Celite pad was washed with heptane, and the organic phase was passed through a short column of SiO_2. Heptane was removed under reduced pressure using a rotary evaporator. The yield was quantitative, and the purity of SQA determined by GC was higher than 98 %.

2.2 Catalysts

Pd/Al_2O_3 (Alfa Aesar, Product number 11713, batch number Z07B031) and Siliacat® Pd catalyst (SiliCycle (Canada), Product number R815-100, batch number 106744) were used directly. Pd/CNT was prepared according to a previous publication [23]. Our groups recently demonstrated that isolated palladium single atoms (Pd_{SA}) and nanoparticles (Pd_{NP}) are simultaneously present on the

carbon support [24, 25]. Pd/CNT catalyst was already characterized by XRD, XPS, and TPD/MS analysis [23, 24]. From the STEM-HAADF analyses, a semi-quantitative Pd_{SA}/Pd_{NP} ratio of ≈ 2 for the Pd/CNT catalyst was determined [24]. The Pd_{SA}/Pd_{NP} ratio (a number ratio) was measured from the STEM-HAADF analyses of at least 500 elements. Table 1 compared the characteristic of the catalysts used in this study, and Figure 2 shows representative STEM-HAADF images of the Pd/CNT catalyst, where isolated Pd_{SA} and Pd_{NP} coexist.

Table 1. Characterization of the catalysts

Catalyst	Metal content (wt %)	Particle size (nm)	Pd dispersion (%)
Pd/Siliacat® [a]	2.13	3.1	n.d.
Pd/Al_2O_3 [b]	5.00	3.9 ± 1.1	31
Pd/CNT [b]	2.04	2.2 ± 1.2	49
Pd/CNT@FeCrAlOY	[c]	2.0 ± 0.5	51

[a] see ref. [26];[b] see ref. [24]; [c] see section 2.5

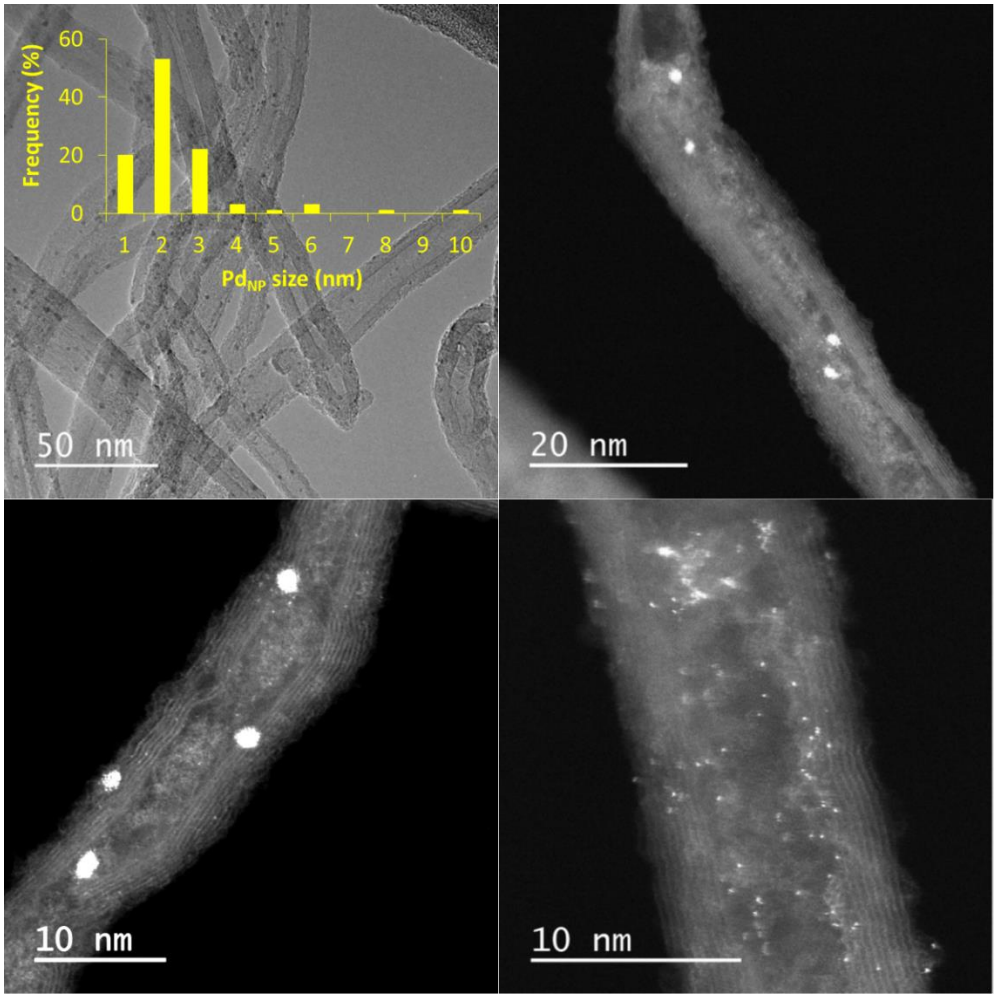

Figure 2. STEM (scale bar = 50 nm) and STEM-HAADF (scale bar = 20 and 10 nm) micrographs of Pd/CNT.

2.3. General procedure for the hydrogenation of SQE in stirred tank reactor

The reactions were performed in a 200 mL thermo-regulated stainless steel autoclave from Top Industrie. Four baffles were mounted to the reactor walls, and the reaction medium was stirred by a gas-inducing impeller having six straight blades. Temperature control is provided by both an electric shell (for heating) and a Ranque-Hilsch vortex device (for cooling). The reactor is operated at constant pressure, in batch mode for the liquid and solid phases and semi-batch mode for the gas phase. Hydrogen was constantly fed via a pressure regulator and supplied by a calibrated reserve. The pressure and temperature monitoring of this reserve over time provide the hydrogen consumption profile.

The catalyst and 80 mL of the desired mixture of SQE and solvent were placed in the reactor. Tetradecane (0.1 M) was used as an internal standard. The reactor was purged with N_2 at room temperature, and the reactor was heated to the desired temperature under stirring. When the desired temperature was reached, the stirring was stopped. The N_2 atmosphere was replaced by H_2 by several purges, and the experiment was started by switching on the agitator. H_2 consumption and liquid phase temperature were recorded as the function of time (1 Hz) using Labview®.

G-L equilibrium flash calculations help estimate solvent vaporization and hydrogen solubility for the heptane/squalene mixtures in the different experimental conditions used in this study (See supporting information, Figures S1 and S2 and Table S1).

2.4. Analytical monitoring of the reaction progress

Unlike other terpenes, the reactivity of the double bonds in SQE is similar (6 tri-substituted double bonds with comparable steric crowding). In addition, there are 4 prochiral carbons in SQE. As such, identifying different intermediates as the function of time by classical GC/FID or GC/MS method is impractical (See supporting information, figure S3 to S5). It was indeed impossible to kinetically measure the first step of the reaction or to perform a proper kinetic study. Nevertheless, reactant (SQE) and product (SQA) could be identified and quantified from the bulk of intermediates using GC/FID using tetradecane as internal standard (I.S.) (See Figures S6 to S8).

However, reaction progress could be easily followed by monitoring H_2 consumption as the function of time. For each experiment, the reaction mixtures were analyzed by GC-FID equipped with DB-17 column and SQE conversion. SQA yield and selectivity could be determined using tetradecane as I.S. . The concentration of intermediates could be determined by the difference between initial SQE and SQA formed.

2.5. Coating procedure of FeCrAlOY foams [27]

FeCrAlOY foams (Holomet Foamet 400 µm, void fraction 92 % and geometrical specific surface area of 7050 m^2/m^3) (See supporting information, Figures S9 and S10, Table S2) were cut in cylinders (∅=4.3 mm and L=50.0 mm) or in rectangular sheets (12 mm x 1.5 mm x 150 mm) through electrical discharge machining [28]. After degreasing with acetone, metallic foam substrates were submitted to a preliminary heat treatment at 500 °C under an air atmosphere for 6 h. After cooling down, the foam pieces were dip-coated with an aqueous suspension of the 2.04 wt% Pd/CNT catalyst (100 g/L) according to the procedure developed in our group [27]. After air blowing and drying, a final heat treatment at 300 °C under a reductive N_2-H_2 mixture provides the final supported catalyst. This procedure obtained a similar mean catalyst mass of Pd/CNT per liter of FeCrAlOY foam, *i.e.*, 17.2 ± 5.0 $g_{Pd/CNT}/L_{foam}$ and 16.5 ± 4.0 $g_{Pd/CNT}/L_{foam}$ for cylinders and rectangular sheets, respectively. Assuming an homogeneous coating of the foam objects, these similar loadings correspond to an estimated mean layer thickness around 4–5 µm. It has been checked that the particle size distribution (2 ± 0.5 nm) and the Pd_{SA}/Pd_{NP} ratio (5.6) of the Pd/CNT catalyst (Figure S5) were not significantly modified by the coating process.

2.6. General procedure for the hydrogenation of SQE in flow

The experimental setup for the hydrogenation of SQE in flow is detailed in Scheme 1. Cylindrical coated foam objects were inserted in a homemade milli-reactor, i.e., 4 tubes in series of 100 mm length and 4.4 mm internal diameter (Figure 3) or in a Miprowa-Lab reactor (8 channels in series of 300 mm length with a width of 12 mm and a height of 1.5 mm).

a)

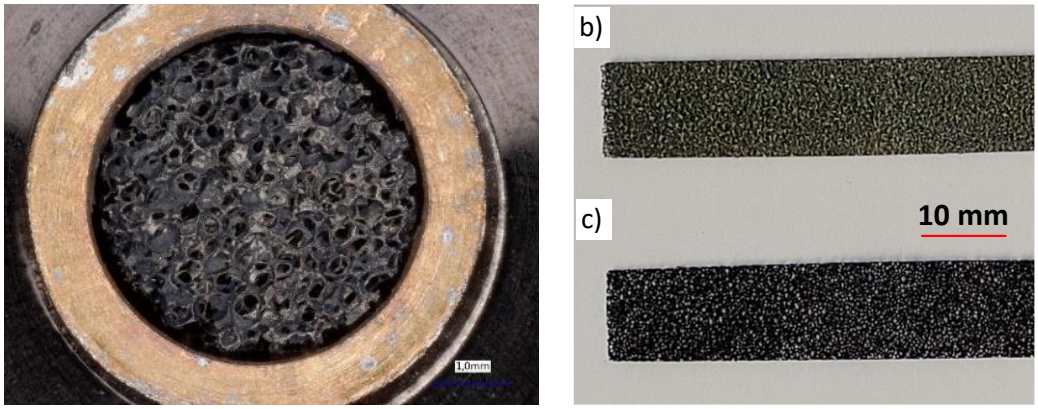

Figure 3. a) Optical microscopy picture of the coated metallic foam inserted into the stainless steel tubing. b) Uncoated foam sheets and c) Coated foam sheets with Pd/CNT catalyst used in Miprowa-lab reactor.

The temperature was controlled by a thermoregulated oven or a heated circulating bath for cylinders and rectangular sheets, respectively (Scheme 1). The temperature inside the reactor was monitored using J-type thermocouples. In a 1000 mL volumetric flask, 0.33 M SQE with tetradecane as internal standard was prepared. At the reactor inlet, organic solution (ensured by an HPLC pump Shimadzu LC 20 AD) and gas flow (regulated by a mass flow controller Bronkhorst Elflow Prestige) meet at a T junction. An Equilibar back pressure regulator precisely regulated outlet pressure. G-L separation and liquid collection are ensured by gravity. When a stable temperature was obtained, periodical analysis of the liquid phase by GC-FID and GC-MS was used to calculate the conversion of SQE and the yield of SQA.

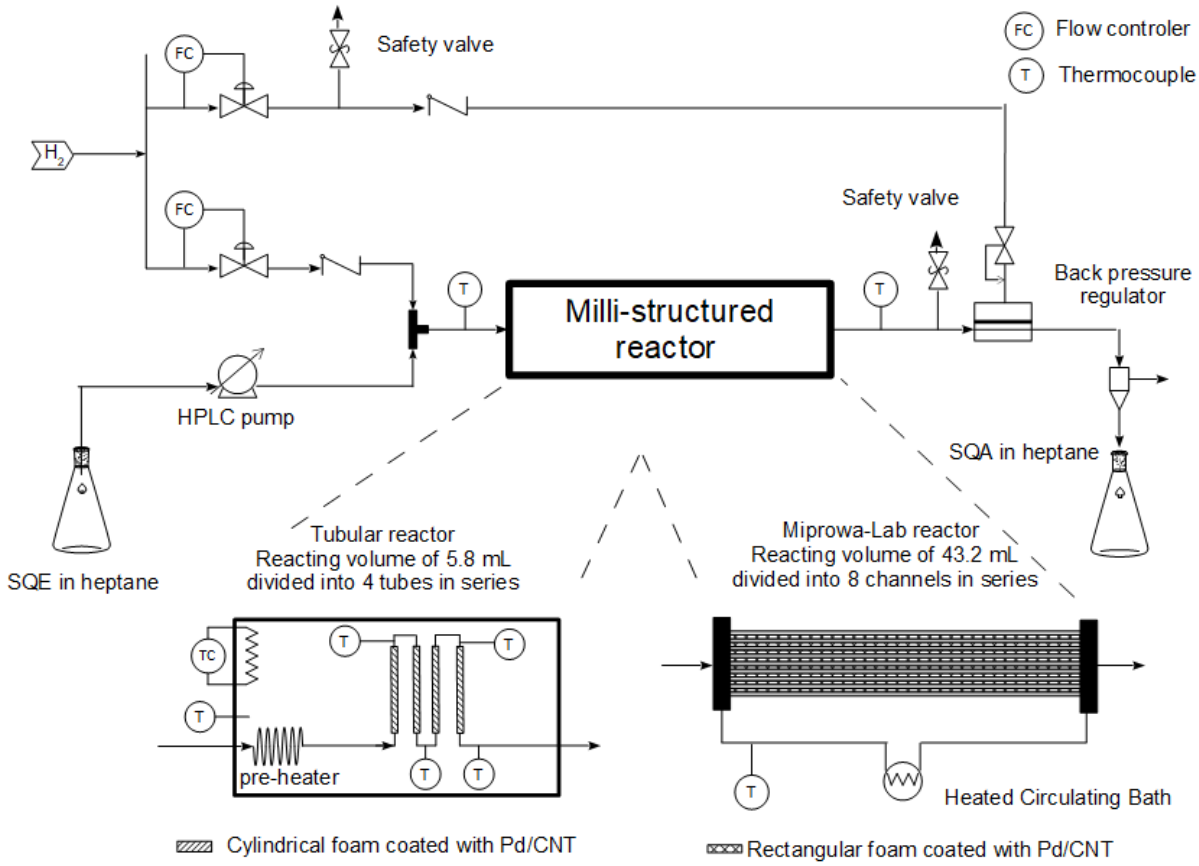

Scheme 1. Experimental setup for the reduction of SQE in flow using milli-reactor

The continuous experiments were performed at 120 °C or 180 °C and 30 bar of H_2, applying a gas flowrate (Q_G) between 200 and 1800 NmL.min^{-1} and liquid flow (Q_L) (SQE 0.3M in heptane) between 1 to 20 mL.min^{-1}. In all experiments, an excess of H_2 was used (H_2/SQE molar ratio between 12 and 40). Periodical analysis of the liquid phase by GC-FID and GC-MS is used to calculate the conversion of SQE, the yield of SQA.

3. Results and discussion

3.1. Hydrogenation of SQE by commercial catalysts

The reduction of SQE was first studied using the commercial Siliacat® Pd catalyst under the experimental conditions (50 °C, H_2 3 bar, Pd/SQE = 0.5 mol % and EtOH as solvent) described by M. Pagliaro *et al*. [18]. Reaction progress could not be easily followed by in-situ or ex-situ analysis. The reactivities of double bonds in SQE are similar and partial reduction could lead to the formation of up to 62 intermediate species and their isomers (See supporting information, Figures S6 to S9 for typical chromatograms). Thus, identifying and quantifying different intermediate species as the function of time by classical GC/FID and GC/MS methods is impractical. However, monitoring H_2 pressure inside the batch reactor as the function of time (Figure 4) could give reliable information on the apparent catalytic activity. When 6 mol of H_2 per mol of SQE are consumed, the reaction was stopped, and analysis of the reaction mixture using GC-FID and GC-MS system, both equipped with DB-17 columns, confirmed the total reduction of SQE into SQA (within the experimental error of 2 %).

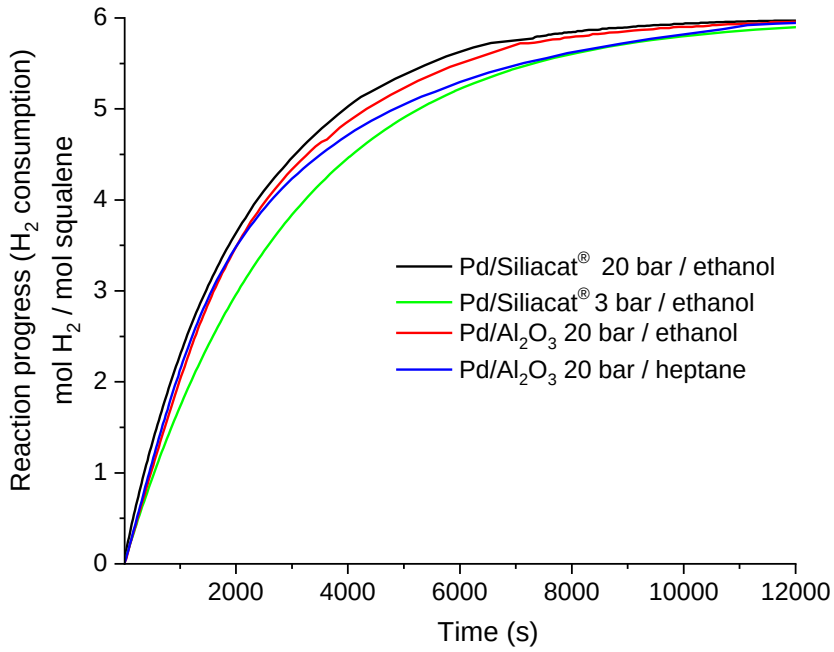

Figure 4. H_2 consumption as the function of time, solvent, catalyst, and H_2 pressure. Reaction conditions: SQE 0.33M in EtOH or heptane, 50 °C, H_2 3 bar or 20 bar, Pd/SQE = 0.5 mol %; Liquid phase 80 mL, 280 mg of 5wt % Pd/Al_2O_3 or 670 mg of 2.1wt % Pd/Siliacat®

Surprisingly, at room temperature, SQE was not fully soluble in EtOH (0.33 M). A milky suspension was formed under stirring that rapidly demixes on standing. Despite the formation of this emulsion, a quantitative yield of SQA was obtained in ~ 3.5 h (Figure 4), as expected from the works of M. Pagliaro *et al*. [18]. An increase of H_2 pressure from 3 to 20 bar slightly increased the initial chemical rate, measured by the hydrogen consumption rate, but does not change the time to get total conversion into SQA, ~3.5 h (12'000 s). Siliacat® Pd catalyst was then compared to a Pd/Al_2O_3 (Strem Chemicals) catalyst using the same metal loading and experimental conditions. A similar H_2 consumption profile was observed, indicating similar reaction progress and chemical rate (Figure 4). The complete hydrogenation was obtained concurrently, in ~3.5 h. In heptane, a suitable solvent for

SQE, similar reactivity was observed (Figure 4). As such, Pd/Al_2O_3 in heptane was chosen as a catalytic reference system to further optimize the reduction of SQE.

3.2. Influence of the temperature on hydrogenation of SQE by commercial catalyst

The influence of the temperature on the catalytic activity was then studied (Figure 5) with the Pd/Al_2O_3 reference catalyst. As expected, the chemical rate, determined by the apparent H_2 consumption rate, was increased with increasing the temperature. After checking for the absence of physical transport limitations and assuming similar reactivity of the six double bonds of SQE (trisubstituted C=C, see Figure 1), the apparent H_2 consumption rate profiles could be regressed using a pseudo-1st order kinetic rate expression regarding the C=C double bonds concentration. The apparent kinetic constant increased sixtyfold from 50 °C to 120 °C, corresponding to an apparent activation energy of 55 $\pm$ 5 kJ.mol^{-1}. A slight decrease of apparent activation energy is noticed above 120°C, most probably meaning the appearance of some internal mass transfer limitation. Consequently, even if present on the figure 5, the point at 140°C was not considered for the apparent activation energy determination. Due to the exothermicity of the total hydrogenation reaction ($\Delta_r H$ = – 765 kJ.mol^{-1}), increased reaction rate means increased heat production rate. However, in the experimental domain tested with this catalyst, the exothermicity was easily handled by the stirred tank reactor and its cooling system up to 120 °C (ΔT ~ 10 °C for the experiment at 120 °C, see Supporting information, Figure S12). The temperature was thus set to 120 °C for the following experiments.

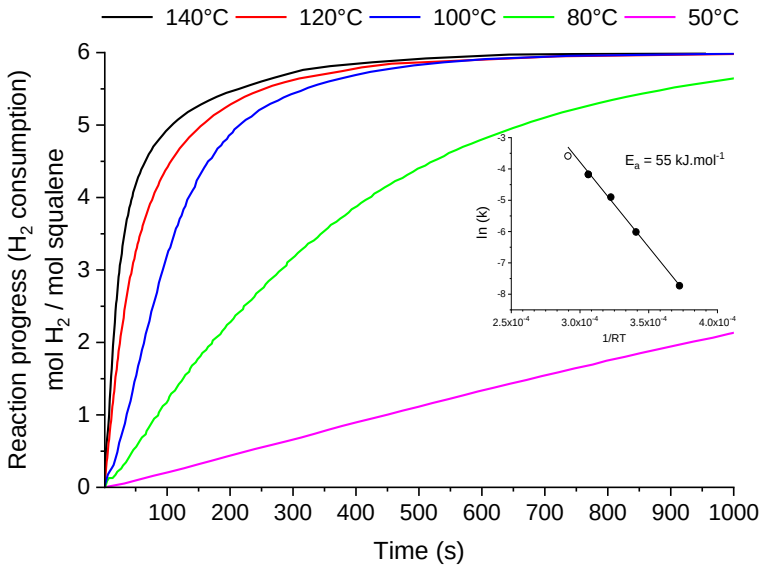

Figure 5. H_2 consumption as the function of the temperature. Reaction conditions: SQE 0.33M in heptane, H_2 20 bar, Pd/SQE = 0.5 mol %; Liquid phase 80 mL, 280 mg of 5wt % Pd/Al_2O_3. Insert: Arrhenius plot of the apparent kinetic constant (k in s^{-1}).

3.3. Influence of the substrate concentration on hydrogenation of SQE by commercial catalyst

The influence of SQE concentration on the extent of reaction and the apparent rate of H_2 consumption was then studied. When increasing the SQE concentration from 0.15 M to 2.03 M (neat), the time needed to achieve complete hydrogenation of SQE increases, and it is noticeable that the apparent H_2 consumption rate profiles (normalized by the SQE concentration, see Figure 4) tend to decrease. This phenomenon has already been reported in the literature and was explained by strong adsorption of SQE and partially hydrogenated products on the catalyst surface, resulting kinetically in a term of inhibition by the reactant on the rate law [18, 29]. The reduction of neat SQE (100 % conversion and 96 % selectivity) could be achieved after ~ 8.6 h (See supporting information, Figure S13) under those relatively mild conditions (120 °C, H_2 20 bar, Pd/SQE = 0.5 mol %). This result is roughly comparable (in terms of activity) to the published result with 2.5 wt % SiliaCat Pd,[26] *i.e.* 100 % conversion and 99 % selectivity after 24h (70 °C, H_2 3 bar, Pd/SQE = 20 mol %). Comparison of the initial reactions rates as the function of the concentration (Figure 6, inset) showed that the

maximum chemical rate was reached for a concentration between 0.15 and 0.33 M. This evolution of reaction rate with the substrate concentration is typical of Langmuir-Hinshelwood kinetics with competitive adsorption between alkenes and hydrogen resulting in inhibition by the substrate. For further experiments, the experimental conditions were set to a concentration of SQE of 0.33 M in heptane, 120 °C, and 20 bar H_2. This concentration allows a compromise between optimal reaction rate and excessive substrate dilution.

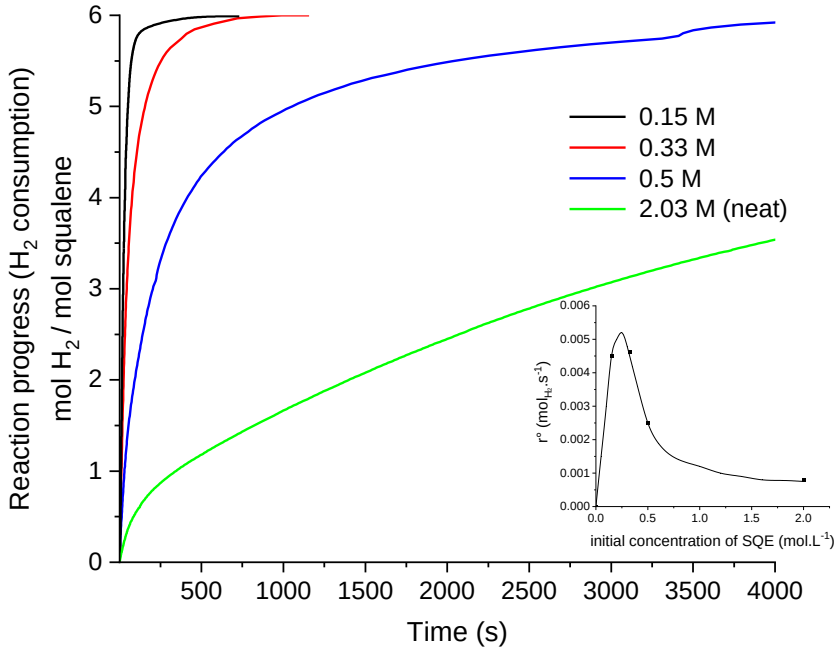

Figure 6. H_2 consumption as the function of the initial concentration of SQE. Reaction conditions: SQE 0.15 M in heptane to 2.03 M (neat), 120 °C, H_2 20 bar, Pd/SQE = 0.5 mol %, 280 mg of 5wt % Pd/Al_2O_3, liquid phase 80 mL. Insert: initial reaction rates (r°) at the function of initial concentration of SQE.

Our groups recently reported that Pd/C catalysts could show high activity for the hydrogenation of monoterpene (β-myrcene) and evidenced a structure-activity correlation, integrating three catalyst structural features: metal dispersion, amounts of surface oxygen groups, and defective sites on the support [23]. While the presence of metal dispersion in such a correlation was not surprising, the

role of surface defects and oxygenated groups was less straightforward. Then, further investigations demonstrated that Pd_{SA} and Pd_{NP} are simultaneously present on the carbon supports and that unique cooperative catalysis operates between these species, allowing one to reach very high apparent activity for monoterpene hydrogenation [24, 25]. Thus, Pd/CNT was evaluated for the reduction of SQE.

3.4. Hydrogenation of SQE in heptane by Pd/CNT catalyst

Pd/CNT catalyst was compared to Pd/Al_2O_3 under the optimized conditions for the latter, *i.e.* SQE 0.33M in heptane, 120 °C 20 bar H_2 (Figure 7), but the Pd/SQE ratio was decreased from 0.5 mol % to 0.2 mol %. Under those conditions, SQE was selectively reduced to SQA in 700 s using Pd/Al_2O_3, whereas less than 120 s were necessary for Pd/CNT (Figure 7). This significant improvement of the catalytic activity is also highlighted by the increase of the liquid phase's temperature (Figure 7). For a SQE concentration of 0.33 M, an adiabatic temperature rise of 160 °C is expected. Despite the use of an efficient Ranque-Hilsch vortex cooling system for this relatively small stirred tank reactor (200 mL), the temperature of the liquid phase reaches 146 °C (ΔT = 26 °C) in less than 20 s for Pd/CNT. This indicates a drastic change in apparent instantaneous activity compared to the reference alumina catalyst, where a lower temperature peak was noticed (ΔT = 10 °C, see Figure 7). Such an abrupt increase of liquid phase temperature has a conjugated effect, accentuating the difference in apparent catalytic activity (Figure 7) as the two parameters are interlinked. Additionally, the performance observed with Pd/CNT could be affected by mass transfer limitation (reactor dependent) at the G-L interface, which was not the case for Pd/Al_2O_3 and Pd/Siliacat® catalysts due to their limited activity. Additional experiments are required with less catalyst to assess a fully quantitative comparison of catalytic activities without any mass or heat transfer limitations. Nevertheless, using the same amount of catalyst (Pd/SQE = 0.2 mol %), total hydrogenation of 0.33 M SQE in heptane could be achieved in less than 120 s with Pd/CNT compared to 900 s with Pd/Al_2O_3 in the same reactor (Figure 7). The coexistence of Pd_{NP} and Pd_{SA} in Pd/CNT catalyst has a synergetic

effect on catalytic activities[25] that have already been discussed for the hydrogenation of monoterpenes [24]. However, the objective of the present work was to intensify the hydrogenation of SQE; thus, new experimental conditions were evaluated.

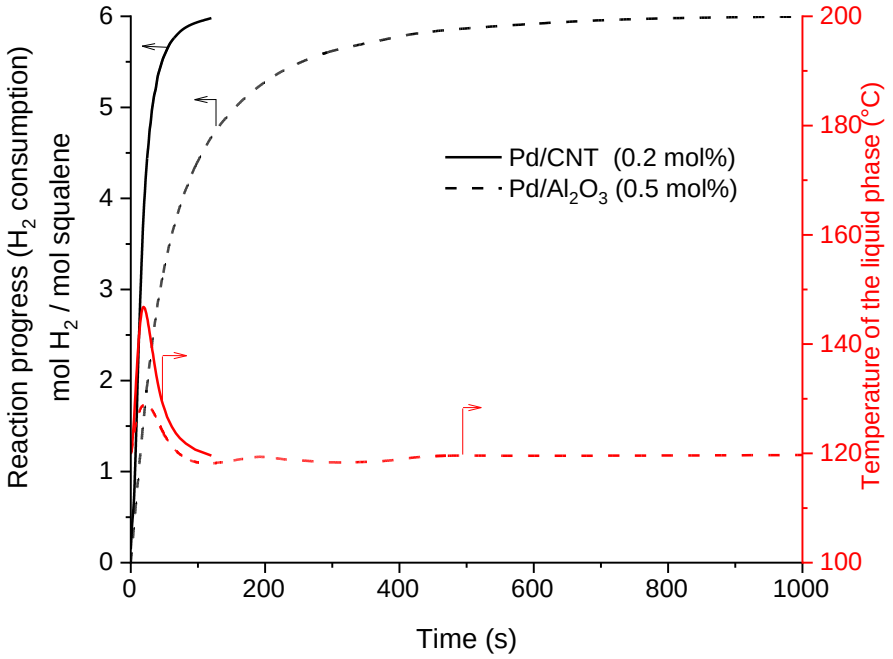

Figure 7. H_2 consumption as the function of time and catalysts. Reaction conditions: SQE 0.33M in heptane; 120 °C; H_2 20 bar; Liquid phase 80 mL; 280 mg 2.04 wt% Pd/CNT (Pd/SQE = 0.2 mol %) or Pd/SQE = 0.5 mol %, 280 mg of 5wt% Pd/Al_2O_3

3.5. Hydrogenation of SQE in SQA by Pd/CNT catalyst

Under previous conditions (Figure 7), post-purification of the product by distillation is necessary (*i.e.* SQA/heptane separation). One way to circumvent this problem is to use the reaction product (*i.e.* SQA) itself as a solvent. SQE was thus dissolved into high purity SQA (> 98 %) to get a concentration of 0.33 M. The comparison between heptane and SQA as the solvent is shown in Figure 8 using 0.2 mol % of Pd/CNT catalyst.

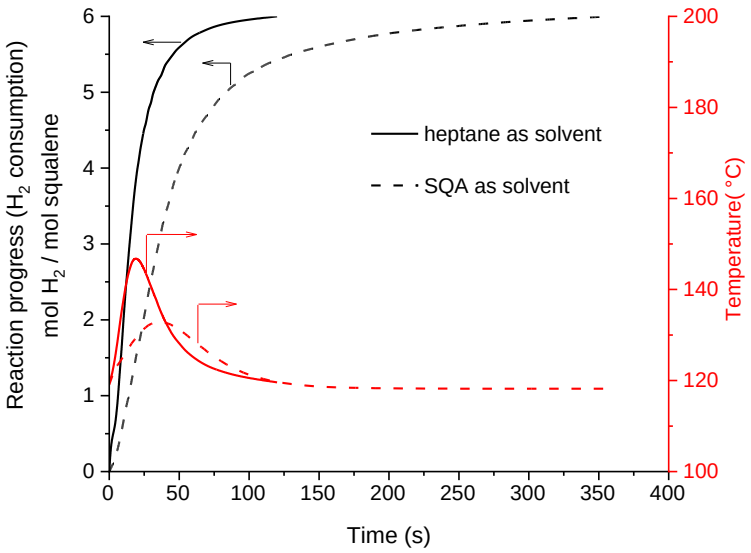

Figure 8. H_2 consumption and temperature of the liquid phase profiles as the function of time and solvent. Reaction conditions: SQE 0.33M in SQA or heptane; 120 °C; H_2 20 bar; Liquid phase 80 mL; Pd/SQE = 0.5 mol%; 280 mg of 2.04 wt% Pd/CNT.

A slight decrease in the apparent activity of the catalyst was noticed using SQA as the solvent compared to heptane (Figure 8). This decrease could be primarily attributed to the decrease of hydrogen solubility from heptane to SQA [30] and an important increase in the solvent's viscosity (0.39 and 36.1 mPa.s^{-1} at 20 °C for heptane and SQA [31] and 2.2 mPa.s^{-1} at 120 °C for SQA [32]). This difference in the apparent catalytic activities is emphasized by the maximum temperature reached by the liquid phase (132 °C *vs.* 146 °C) for SQA and heptane as the solvent, respectively. Still, after 6 min, neat SQA (selectivity > 99.6 %) could be obtained in this stirred tank reactor, and a simple filtration is used to remove the heterogeneous catalyst from the mixture that does not need further purification steps.

3.6. Transposition of batch to continuous flow

Multiphase stirred tank reactors often suffer from safety and productivity issues when scale-up is addressed with such exothermic demanding reactions [33, 34]. Indeed, for given conditions, often optimized at lab-scale, a direct scale-up lead to a significant decrease in available heat transfer capacity (UA_{th}) as the function of the volume of the reactor(V_R), leading thus to highly probable thermal runaway and deteriorated product quality (Figure 9). Reduced and "degraded" experimental windows involving diluted charges or controlled fed-batch operation are used to mitigate this issue but at the extent of an ineluctably reduced reactor productivity and possible extra purification costs.

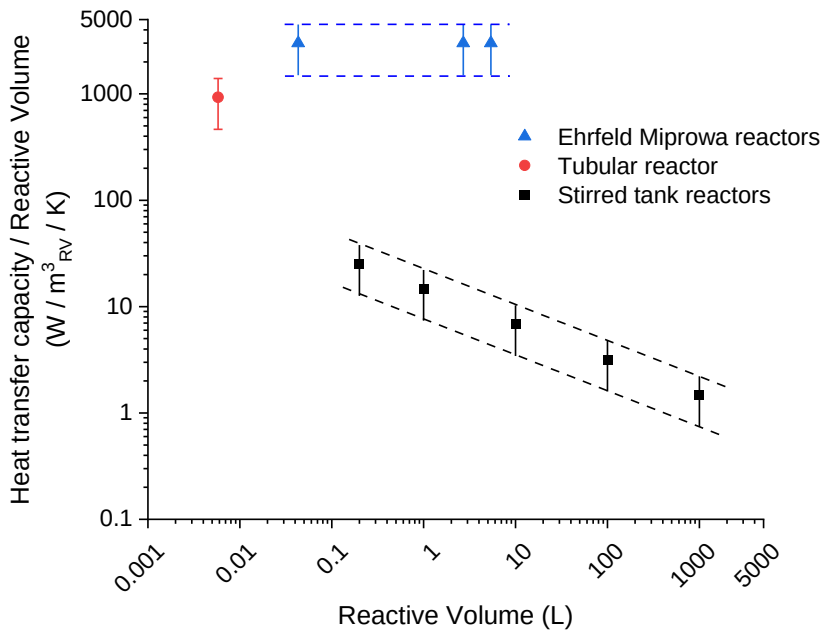

Figure 9. Graphical comparison of the wall heat transfer capacity (UA_{th}) with reacting volume (V_R) for the 3 reactor technologies considered in this study. See Supporting information and Table S3 for details on the methodology used to compare these 3 types of reactors.

It is interesting to notice in this rough comparison that the MIPROWA reactors and the lab-scale tubular foam reactor clearly exceed the stirred tanks, whatever their volume. Moreover, and as

already known, stirred tank vessels see their heat transfer capacity drastically decrease when reactor volume increases while the MIPROWA technologies maintain a constant heat transfer capacity throughout the scaled-up versions due to seamless scale-up consideration.

Due to a similar millimeter-scale geometry and a less efficient external heat transfer coefficient on the utility side, the lab-scale tubular reactor lies slightly behind the MIPROWA reactor but surpasses the stirred tanks. This comparison clearly deserves the interest of such reactors and transpositions for demanding reactions and strengthens the methodology followed in this work.

A novel approach has been proposed for several years with continuous intensified reactor technologies [33, 35, 36]. These reactors allow fast transpositions from traditional lab-scale stirred tank reactors due to small characteristic lengths and more intense physical phenomena (mixing, heat, and mass transfer). Furthermore, extended or new process windows can be reached beyond the batch to continuous transposition, allowing to expect more process intensification of the synthesis [37, 38]. Finally, with the more and more mature “seamless scale up” strategy [39-41], identical physical performances are provided at different production capacities (Figure 9) up to the industrial one, ensuring an easy and quasi instantaneous scale up.

Pd/CNT appears as a nano-textured micro powder (particle size < 10 μm), and its processability in continuous equipment appears as a bottleneck. Micropacked bed reactors have been successfully demonstrated [42, 43] for such 3-phase operations but were operated with larger particles (10-100μm), and prohibitive pressure drops are expected with this catalyst. “Slurry Taylor flow”, already mastered in our group [44-46], can be envisaged as an advantageous contacting mode, but its scalability remains unsolved.

Recently, the design of 3D printed supports for continuous reactors has been described [22, 47-49], particularly for SQE reduction [22]. The catalyst could be prepared by electrodeposition [47], impregnation [22], and coating with a supported catalyst layer [48, 49]. The catalyst immobilization on metallic open cell foams (OCF) has been developed in our group for several years [50, 51] and has

been favored here to operate this catalyst in continuous flow mode. OCF have several attractive benefits compared to 3D printed supports. OCF are structured materials commercially available at a relatively low cost. This structure can present interesting features such as high thermal conductivity, appropriate mixing due to the disordered structure, low-pressure drop, and large external specific surface area (up to 10,000 m^2/m^3). OCF have demonstrated their interest as heat exchangers, internal mixers, and catalyst supports by the past [50, 51]. Metallic OCF offers a good cutting accuracy (±5 μm) by electro-machining discharge, ensuring then a perfect adaptation to the geometry of the different types of flow reactors without any wall by-pass issues. Finally, foam internals can be prepared for a wide range of reactor diameters (millimetre-scale to decimetre-scale) and cross sections.

A first lab-scale transposition with millimeter-scale cylindrical FeCrAlOY foam objects (∅ = 4.3 mm) inserted in 4 stainless steel tubing ((∅ = 4.4 mm, L = 100 mm) was undertaken (Scheme 1). Such a small millimeter-scale allows the use of a reasonable reactant (and solvent) inventory (active reactor volume of 5.8 mL with a total catalyst amount of 0.1 g) for a lab-scale demonstration combined with the benefits of good heat and mass transfers capacities (Figure 9).

Periodical analysis of the liquid phase at the reactor outlet by GC-FID and GC-MS is used to determine the concentration profile of SQE, the yield of SQA at 120 °C, and 30 bar of H_2 as the function of contact time is reported in Figure 10. Contact time was defined as the ratio of the reactor volume (V_r) *vs.* the liquid phase flow (Q_L). For this experiment, a constant large excess of hydrogen was used (H_2/SQE molar ratio of 30), *i.e.* the hydrogen flow (Q_G) *vs.* Q_L was kept constant. Total conversion of SQE was obtained for a contact time below 1 min (Figure 10). When increasing the contact time, *i.e.* decreasing Q_L, the concentration of SQA at the reactor outlet rapidly increases (Figure 10, and Table 2, entries 1-3). Quantitative yields (SQA > 99%) were obtained for a contact time of 6 min (Table 2, entry 3) with a space-time yield of 17 $mol_{SQA}.mol_{Pd}^{-1}.min^{-1}$(Table 2, entry 3).

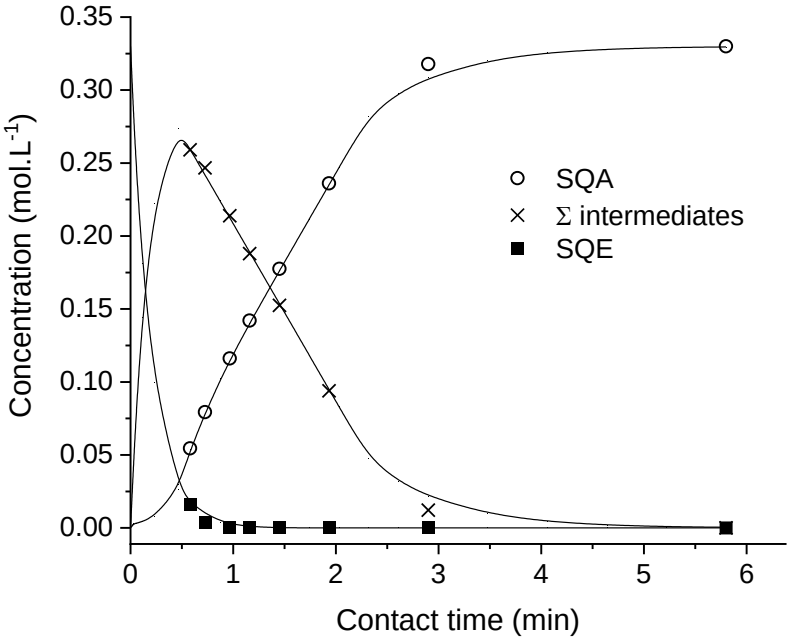

Figure 10. Concentration at the reactor outlet as the function of contact time for the hydrogenation of SQE in flow using tubular reactor. Reaction conditions: SQE 0.33 M in heptane; 120 °C, H_2 30 bar; Q_G/G_L = 10; H_2/SQE molar ratio = 30; 0.10 g of 2.04 wt% Pd/CNT coated on 400 µm foams; foam volume : 5.8 mL; SQA and SQE concentration were determined by GC/FID using internal calibration. The concentration of the different intermediates was calculated by the difference in the concentration of SQA and SQE. Lines are guides to the eyes.

The absence of external mass transfer limitation was checked by using 3 different lengths of reactor. For the same contact time (V_R/Q_L), both conversion and yield were identical for those 3 different reactors (see Supporting information, Figure S14). The hydrogen flow (Q_G) has little impact on the mean liquid residence time [51, 52] and in conversion and selectivity levels since no mass transfer limitation was detected, as far as hydrogen is provided in excess (an H_2/SQE molar ratio between 24 and 237 was used).

Table 2. SQA yield and Space-Time Yield (STY) as the function of temperature and contact time in the tubular reactor

Entry	Temperature (°C)	Contact time (min) [b]	SQA Yield % [c]	STY ($mol_{SQA}.mol_{Pd}^{-1}.min^{-1}$)
1	120	1.9	72	37
2	120	2.9	94	32
3	120	5.8	> 99	17
4	180	0.7	85	117
5	180	1.0	96	96
6	180	1.45	> 99	68

[a] Reaction conditions: SQE 0.33 M in heptane; 120 °C or 180 °C, H_2 30 bar; H_2/SQE molar ratio = 30; 0.10 g of 2.04 wt% Pd/CNT coated on 400 µm foams; reactor volume : 5.8mL.

[b] Contact time = V_r/Q_L

[c] SQA yield was determined by GC-FID using internal standard

Then, in an attempt to further improve the continuous reactor productivity, the temperature was increased to 180 °C (see Supporting information, Figure S15). The productivity increases reaching a space-time yield of up to 117 $mol_{SQA}.mol_{Pd}^{-1}.min^{-1}$ (Table 2, entry 4) for a SQA yield of 85%. In order to increase the SQA yield, the contact time was increased. Fully reduced SQA (> 99 %) was obtained at 180 °C and 30 bar of H_2 for a contact time of 1.45 min (Entry 6, Table 2) with a space-time yield of 68 $mol_{SQA}.mol_{Pd}^{-1}.min^{-1}$ and volumetric productivity of 95.3 kg of fully reduced SQA (> 99 %) per liter of reactor and per minute. It is worth noting that under those conditions, the reaction rate is partially limited by mass transfers; thus, the yield improvement is much lower compared to what could be expected on a chemical kinetic basis. Moreover, only a minor improvement can be expected by increasing further the reaction temperature.

At 180 °C, a low exothermicity could be detected inside the reactor (see Supporting information, Figure S16), illustrating one significant benefit of this contact mode. The observed exothermic peak

remains below 10 °C (ΔT_{max}=7 °C) inside the reactor and was dependent on the liquid flow rate (Q_L): The temperature profile tends to spread and flatten when increasing liquid flowrate as expected.

Catalyst stability is under evaluation to reach high Turn Over Numbers (TON). This aspect is mandatory for a reliable and robust continuous catalytic process with an immobilized catalyst.

3.7. Seamless scale-up

After this successful batch to continuous transposition at lab-scale, a further step towards a reliable continuous pilot production has been attempted. The scale-up and adaptation of the coated foam inside millimeter-scale tubing (5.8 mL) to a commercially available milli-structured intensified pilot-scale reactor has been done with the Miprowa-Lab reactor (active reactor volume of 43.2 mL with a total catalyst amount of 0.75g) from Ehrfeld Mikrotechnik [53] (Scheme 1, Figure 11). As a result, a potential scale-up factor of 7.5 has been experienced.

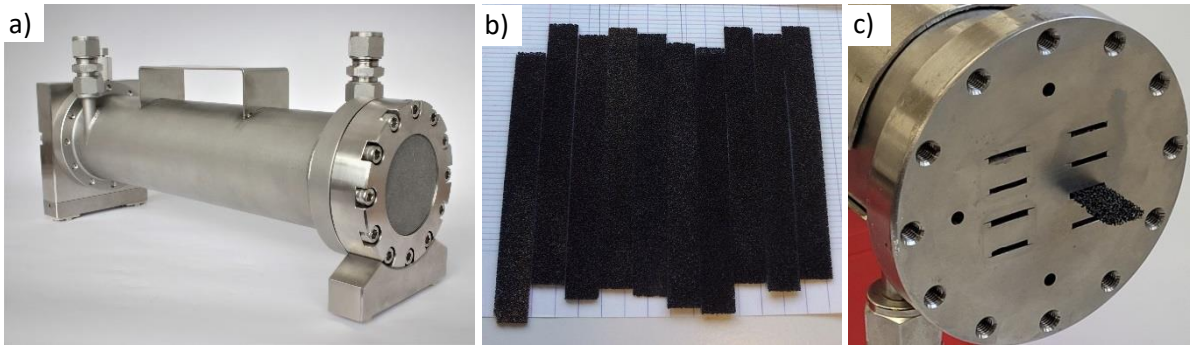

Figure 11. a) Erhfeld Mikrotechnik Miprowa-Lab reactor; b) coated foam internals; c) head of the reacting zone of Erhfeld Mikrotechnik Miprowa-Lab reactor showing the filling with a foam sheet internal.

The reactor's eight millimeter-scale channels (a rectangular cross-section of 12 x 1.5 mm2 x 300 mm length) were easily mounted with coated foam sheets (12 x 1.5 x 150 mm^3) in place of the classical static mixing elements of this technology [49, 53]. The foam material and the coating procedure were identical to the former reactor and led to a roughly similar loading of 16 g of Pd/CNT catalyst per L of foam. As expected, experiments conducted at an iso-contact time and identical process

conditions (120 °C, 30 bar H_2 pressure, and 0.33 M SQE in heptane) demonstrate the successful scale-up from the tubular lab-reactor to this pilot technology. By increasing the liquid flow rate (Q_L) by a factor of 10 by switching from the tubular reactor to the pilot reactor, it is possible to obtain an SQA yield higher than 99% with similar productivity (Table 3, Figure S19 and S20). Under those mild conditions (*i.e.,* 120°C and 30 bar of H_2), a production capacity of 1.989 kg per day using a commercial intensified reactor with a reacting volume of 43.2 mL was obtained (Table 3).

Table 3. Comparison of SQA yield and productivity obtained with tubular reactor (active reactor volume of 5.8 mL) and Miprowa-Lab reactor (active reactor volume of 43.2 mL) under the same operating conditions.[a]

Reactor (vol.)	Temp./P H_2 (°C/bar)	Contact time [b] (min)	Q_L (mL/min)	SQA Yield [c] (%)	SQA Production capacity (kg_{SQA}/day)	Productivity ($kg_{SQA}/m^3_R/min$)
Tubular	120/30	1.9	3 [d]	72		52.0
(5.8mL)	120/30	5.8	1 [e]	> 99	0.199	23.8
Miprowa-Lab	120/30	2.2	20 [f]	63		40.7
(43.2 mL)	120/30	4.3	10 [f]	> 99	1.989	32.0

[a] Reaction conditions: SQE 0.33 M in heptane, 120 °C, H_2 30 bar; 2.04 wt% Pd/CNT coated on FeCrAlOY metallic foams (Foamet 400µm). Catalyst content of 16.5 g and 17.2 g of Pd/CNT per L of reactor (L_R) for tubular and Miprowa-Lab reactor, respectively. [b] Contact time = V_r/Q_L.[c)] SQA yield was determined by GC-FID using internal standard. [d)] Q_G = 800 NmL / min. [e)] Q_G = 200 NmL / min. [f)] Q_G = 1800 NmL / min.

The combination of similar reactor characteristic lengths, comparable catalyst contents, and of course, similar contacting modes with sufficient heat and mass transfer capacities ensured the observed chemical regime operation. It explained the easy scalability of the homemade tubular reactor to this commercial pilot unit. Such a demonstration is useful to promote the maturity of continuous micro/milli structured reactor technologies. The seamless scale-up praised by the provider could then ensure a quasi-instantaneous scale-up to more significant and qualified units suitable to process desired industrial capacities, even for this kind of complex 3-phase chemistries involving new heterogeneous catalysts. Further intensification with novel process windows unreachable safely in large batch stirred tank reactors remains possible and is under study with these continuous tools.

4. Conclusion

High purity SQE, obtained by fermentation using genetically modified yeast, will become an interesting bio-based intermediate over the next few years. To increase the stability and commercial interest of SQE, its efficient reduction into SQA has to be achieved. Selective SQE reduction into SQA can be performed using a classical lab-scale stirred tank reactor (200 mL) under relatively mild conditions (0.33 M, 120 °C, 20 bar H_2, Pd/SQE = 0.2 mol %) using commercially available catalysts.

The use of new Pd/CNT catalysts significantly improves chemical rate under those conditions thanks to the cooperativity between Pd_{NP} and Pd_{SA} [24]. However, the productivity and operability of the lab-scale stirred tank reactor using this very active catalyst are limited by the reaction's exothermicity ($\Delta_r H$= - 765 kJ.mol^{-1}).

The use of the highly active catalyst in flow was investigated by coating it on open-cell solid foam internal, enabling the control of the reaction's exothermicity and further process intensification. At 180 °C and 30 bar of H_2, fully reduced SQA could be obtained without being bothered by the exothermicity of the reaction. Under those conditions, SQE can be reduced into SQA (> 99%) with a contact time of 1.45 min with a space-time yield of 68 $mol_{SQA}.mol_{Pd}^{-1}.min^{-1}$. A step towards a reliable continuous pilot production was taken by implementing the reaction in a commercially available milli-structured intensified pilot-scale reactor. Similar productivity with SQA yields higher than 99%, close to 30 kg of SQA per m^3 of reactor active volume and per min were obtained. These new Pd-supported catalysts meet the need to increase catalytic activity for highly demanding substrates like SQE. Moreover, easy transposition and scalability of the contacting mode to commercial milli-structured reactor have been demonstrated.

Declaration of Competing Interest

The authors declare that they have no known competing financial interests or personal relationships that could have influenced the work reported in this paper.

Acknowledgments

Part of this work was performed within the framework of the "DEEPER" project funded by the region Auvergne-Rhône-Alpes (contract number 15 021131 01 – CNR006) through the 20th FUI call. Part of this work was also supported by the Agence Nationale de la Recherche (ANR project ANR-19, COMET), which is gratefully acknowledged.

Frédéric Bornette and Fabrice Campoli are acknowledged for contributing to the reactor design, fabrication, and instrumentation. Marie-Line Zanota is acknowledged for the characterization of OCF using X-ray tomography and image analysis.

Ehrfeld Mikrotechnik was greatly thanked for the loan of the Miprowa-Lab reactor (www.ehrfeld.com/home.html).

Abbreviations

SQE, squalene; SQA, squalene; CNT, carbon nanotubes; Pd_{SA}, palladium single atoms; Pd_{NP}, nanoparticles; USD, US dollar; GC-FID, Gas Chromatography with Flame-Ionization Detection; GC-MS, Gas Chromatography Mass Spectrometry

Appendix A. Supplementary data

Supplementary data to this article can be found online at https://doi.org/

References

[1] M. Spanova, G. Daum, Squalene - biochemistry, molecular biology, process biotechnology, and applications, Eur. J. Lipid Sci. Technol. 113 (2011) 1299-1320. https://doi.org/10.1002/ejlt.201100203

[2] M. Tsujimoto, A highly unsaturated hydrocarbon in shark liver oil, J. Ind. Eng. Chem. 8 (1916) 889-896. https://doi.org/10.1021/i500010a005

[3] M.A. Lozano-Grande, S. Gorinstein, E. Espitia-Rangel, G. Dávila-Ortiz, A.L. Martínez-Ayala, Plant Sources, Extraction Methods, and Uses of Squalene, Int. J. Agron. (2018) Article ID 1829160. https://doi.org/10.1155/2018/1829160

[4] E. Naziri, F. Mantzouridou, M.Z. Tsimidou, Recovery of Squalene from Wine Lees Using Ultrasound Assisted Extraction—A Feasibility Study, J. Agric. Food. Chem. 60 (2012) 9195-9201. https://doi.org/10.1021/jf301059y

[5] E. Naziri, F. Mantzouridou, M.Z. Tsimidou, Squalene resources and uses point to the potential of biotechnology, Lipid Technology 23 (2011) 270-273. https://doi.org/10.1002/lite.201100157

[6] A. Patel, L. Mu, Y. Shi, U. Rova, P. Christakopoulos, L. Matsakas, Novel Biorefinery Approach Aimed at Vegetarians Reduces the Dependency on Marine Fish Stocks for Obtaining Squalene and Docosahexaenoic Acid, ACS Sustainable Chem. Eng. 8 (2020) 8803-8813. https://doi.org/10.1021/acssuschemeng.0c02752

[7] W. Xu, X. Ma, Y. Wang, Production of squalene by microbes: an update, World J. Microbiol. Biotechnol. 32 (2016) 195. https://doi.org/10.1007/s11274-016-2155-8

[8] L.J. Wei, S. Kwak, J.J. Liu, S. Lane, Q. Hua, D.H. Kweon, Y.S. Jin, Improved squalene production through increasing lipid contents in Saccharomyces cerevisiae, Biotechnol. Bioeng. 115 (2018) 1793-1800. https://doi.org/10.1002/bit.26595

[9] G.P. Ghimire, N.H. Thuan, N. Koirala, J.K. Sohng, Advances in Biochemistry and Microbial Production of Squalene and Its Derivatives, J. Microbiol. Biotechnol. 26 (2016) 441-451. https://doi.org/10.4014/jmb.1510.10039

[10] K. Fisher, F.X. Woolard, Preparation of farnesene dimers and/or farnesane dimers and lubricant compositions thereof, Amyris Biotechnologies, Inc., USA . 2010, Patent WO2010/042208.

[11] K. Fisher, S.J. Schofer, D. Kane, B., Squalane and isosqualane compositions and methods for preparing the same, Amyris Biotechnologies, Inc., USA . 2011, Patent WO 2011/146837.

[12] E. Naziri, R. Consonni, M.Z. Tsimidou, Squalene oxidation products: Monitoring the formation, characterisation and pro-oxidant activity, Eur. J. Lipid Sci. Technol. 116 (2014) 1400-1411. https://doi.org/10.1002/ejlt.201300506

[13] S. Sabetay, Cinq années de perhydrosqualène, Rev. Fr. Corps Gras 1 (1956) 26-30.

[14] S.L. Bang, J. Bucciero, C. Elmasry, Hydrating cosmetic composition comprising glycerin, alkanediol, emollient, and surfactant, L'Oreal, Fr., 2014, Patent WO 2014/033640.

[15] A. García-Trenco, E.R. White, A. Regoutz, D.J. Payne, M.S.P. Shaffer, C.K. Williams, Pd_2Ga-Based Colloids as Highly Active Catalysts for the Hydrogenation of CO_2 to Methanol, ACS Catal. 7 (2017) 1186-1196. https://doi.org/10.1021/acscatal.6b02928

[16] C. Méhault, L. Vanoye, R. Philippe, C. de Bellefon, Multiphase alternated slug flows: Conditions to avoid coalescence and characterization of mass transfer between droplets, Chem. Eng. J. 407 (2021). https://doi.org/10.1016/j.cej.2020.127215

[17] D.C. Gary, M.W. Terban, S.J.L. Billinge, B.M. Cossairt, Two-Step Nucleation and Growth of InP Quantum Dots via Magic-Sized Cluster Intermediates, Chem. Mater. 27 (2015) 1432-1441. https://doi.org/10.1021/acs.chemmater.5b00286

[18] V. Pandarus, R. Ciriminna, S. Kaliaguine, F. Beland, M. Pagliaro, Heterogeneously Catalyzed Hydrogenation of Squalene to Squalane under Mild Conditions, ChemCatChem 7 (2015) 2071-2076. https://doi.org/10.1002/cctc.201402668

[19] A. Kaiya, T. Nakamura, H. Wada, Highly pure squalane, raw material for pharmaceuticals and cosmetics prepared by using the same and method for producing the same, Nippon Petrochemicals Compagny, Inc., Japan, 2000, US Patent 6,165,481.

[20] J. Dale, T. Artun, Double bond migration and dehydrogenation of squalene on hydrogenation catalysts, Acta Chem. Scand. 10 (1956) 439-444. https://doi.org/10.3891/acta.chem.scand.10-0439

[21] R. Ciriminna, V. Pandarus, F. Beland, M. Pagliaro, Catalytic Hydrogenation of Squalene to Squalane, Org. Process Res. Dev. 18 (2014) 1110-1115. https://doi.org/10.1021/op5002337

[22] S. García, S. Poulston, D. Modeshia, P. Stavarek, M. Ujcic, F. Lali, M.A. Alves, J.D. Araújo, M. Krusche, F. Ullrich, D. Maier, Continuous Production of Squalane Using 3D Printed Catalytic Supports, Johnson Matthey Technol. Rev. 63 (2019) 191-204. https://doi.org/10.1595/205651319X15535963555844

[23] R.C. Contreras, B. Guicheret, B.F. Machado, C. Rivera-Cárcamo, M.A. Curiel Alvarez, B. Valdez Salas, M. Ruttert, T. Placke, A. Favre-Réguillon, L. Vanoye, C. de Bellefon, R. Philippe, P. Serp, Effect of mesoporous carbon support nature and pretreatments on palladium loading, dispersion and apparent catalytic activity in hydrogenation of myrcene, J. Catal. 372 (2019) 226-244. https://doi.org/10.1016/j.jcat.2019.02.034

[24] C. Rivera-Cárcamo, I.C. Gerber, I. del Rosal, B. Guicheret, R. Castro Contreras, L. Vanoye, A. Favre-Réguillon, B.F. Machado, J. Audevard, C. de Bellefon, R. Philippe, P. Serp, Control of the single atom/nanoparticle ratio in Pd/C catalysts to optimize the cooperative hydrogenation of alkenes, Catal. Sci. Technol. 11 (2021) 984-999. https://doi.org/10.1039/D0CY01938K

[25] P. Serp, Cooperativity in supported metal single atom catalysis, Nanoscale 13 (2021) 5985-6004. https://doi.org/10.1039/d1nr00465d

[26] V. Pandarus, R. Ciriminna, F. Beland, M. Pagliaro, S. Kaliaguine, Solvent-Free Chemoselective Hydrogenation of Squalene to Squalane, ACS Omega 2 (2017) 3989-3996. https://doi.org/10.1021/acsomega.7b00625

[27] F. Simescu-Lazar, T. Chaieb, S. Pallier, L. Veyre, R. Philippe, V. Meille, Direct coating of carbon-supported catalysts on monoliths and foams – Singular behaviour of Pd/MWCNT, Appl. Catal., A 508 (2015) 45-51. https://doi.org/10.1016/j.apcata.2015.09.042

[28] EDM Précision, 69100 Villeurbanne, France. https://www.edm-precision-lyon.fr/ (accessed 22 September 2021).

[29] V.K. Soni, R.K. Sharma, Palladium-Nanoparticles-Intercalated Montmorillonite Clay: A Green Catalyst for the Solvent-Free Chemoselective Hydrogenation of Squalene, ChemCatChem 8 (2016) 1763-1768. https://doi.org/10.1002/cctc.201600210

[30] K.J. Kim, T.R. Way, K.T. Feldman, A. Razani, Solubility of Hydrogen in Octane, 1-Octanol, and Squalane, J. Chem. Eng. Data 42 (1997) 214-215. https://doi.org/10.1021/je960268z

[31] M.J.P. Comuñas, X. Paredes, F.M. Gaciño, J. Fernández, J.P. Bazile, C. Boned, J.L. Daridon, G. Galliero, J. Pauly, K.R. Harris, M.J. Assael, S.K. Mylona, Reference Correlation of the Viscosity of Squalane from 273 to 373 K at 0.1 MPa, J. Phys. Chem. Ref. Data 42 (2013) 033101. https://doi.org/10.1063/1.4812573

[32] S.K. Mylona, M.J. Assael, M.J.P. Comuñas, X. Paredes, F.M. Gaciño, J. Fernández, J.P. Bazile, C. Boned, J.L. Daridon, G. Galliero, J. Pauly, K.R. Harris, Reference Correlations for the Density and Viscosity of Squalane from 273 to 473 K at Pressures to 200 MPa, J. Phys. Chem. Ref. Data 43 (2014) 013104. https://doi.org/10.1063/1.4863984

[33] Z. Anxionnaz, M. Cabassud, C. Gourdon, P. Tochon, Heat exchanger/reactors (HEX reactors): Concepts, technologies: State-of-the-art, Chemical Engineering and Processing: Process Intensification 47 (2008) 2029-2050. https://doi.org/10.1016/j.cep.2008.06.012

[34] N. Kockmann, M. Gottsponer, Heat Transfer Limitations of Gas-Liquid Exothermic Reactions in Microchannels, ASME 2010 8th International Conference on Nanochannels, Microchannels, and Minichannels, 2010, pp. 193-199. https://doi.org/10.1115/fedsm-icnmm2010-30389

[35] P. Plouffe, A. Macchi, D.M. Roberge, From Batch to Continuous Chemical Synthesis—A Toolbox Approach, Org. Process Res. Dev. 18 (2014) 1286-1294. https://doi.org/10.1021/op5001918

[36] F. Théron, Z. Anxionnaz-Minvielle, M. Cabassud, C. Gourdon, P. Tochon, Characterization of the performances of an innovative heat-exchanger/reactor, Chemical Engineering and Processing: Process Intensification 82 (2014) 30-41. https://doi.org/10.1016/j.cep.2014.04.005

[37] V. Hessel, Novel Process Windows - Gate to Maximizing Process Intensification via Flow Chemistry, Chem. Eng. Technol. 32 (2009) 1655-1681. https://doi.org/10.1002/ceat.200900474

[38] T. Illg, P. Lob, V. Hessel, Flow chemistry using milli- and microstructured reactors-from conventional to novel process windows, Bioorg. Med. Chem. 18 (2010) 3707-3719. https://doi.org/10.1016/j.bmc.2010.03.073

[39] E.D. Lavric, P. Woehl, Advanced-Flow™ glass reactors for seamless scale-up, Chimica Oggi 27 (2009) 45-48.

[40] A. Steiner, P.M.C. Roth, F.J. Strauss, G. Gauron, G. Tekautz, M. Winter, J.D. Williams, C.O. Kappe, Multikilogram per Hour Continuous Photochemical Benzylic Brominations Applying a Smart Dimensioning Scale-up Strategy, Org. Process Res. Dev. 24 (2020) 2208-2216. https://doi.org/10.1021/acs.oprd.0c00239

[41] A. Potdar, L.C.J. Thomassen, S. Kuhn, Scalability of 3D printed structured porous milli-scale reactors, Chem. Eng. J. 363 (2019) 337-348. https://doi.org/10.1016/j.cej.2019.01.082

[42] M.W. Losey, M.A. Schmidt, K.F. Jensen, Microfabricated Multiphase Packed-Bed Reactors: Characterization of Mass Transfer and Reactions, Ind. Eng. Chem. Res. 40 (2001) 2555-2562. https://doi.org/10.1021/ie000523f

[43] M. Irfan, T.N. Glasnov, C.O. Kappe, Heterogeneous Catalytic Hydrogenation Reactions in Continuous-Flow Reactors, ChemSusChem 4 (2011) 300-316. https://doi.org/10.1002/cssc.201000354

[44] A.-K. Liedtke, F. Bornette, R. Philippe, C. de Bellefon, External liquid solid mass transfer for solid particles transported in a milli-channel within a gas–liquid segmented flow, Chem. Eng. J. 287 (2016) 92-102. https://doi.org/10.1016/j.cej.2015.10.109

[45] A. Ufer, D. Sudhoff, A. Mescher, D.W. Agar, Suspension catalysis in a liquid–liquid capillary microreactor, Chem. Eng. J. 167 (2011) 468-474. https://doi.org/10.1016/j.cej.2010.09.088

[46] F. Salique, A. Musina, M. Winter, N. Yann, P.M.C. Roth, Continuous Hydrogenation: Triphasic System Optimization at Kilo Lab Scale Using a Slurry Solution, Front. Chem. Eng. 3 (2021) 701910. https://doi.org/10.3389/fceng.2021.701910

[47] A. Avril, C.H. Hornung, A. Urban, D. Fraser, M. Horne, J.P. Veder, J. Tsanaktsidis, T. Rodopoulos, C. Henry, D.R. Gunasegaram, Continuous flow hydrogenations using novel catalytic static mixers inside a tubular reactor, React. Chem. Eng. 2 (2017) 180-188. https://doi.org/10.1039/c6re00188b

[48] M. Kundra, T. Grall, D. Ng, Z. Xie, C.H. Hornung, Continuous Flow Hydrogenation of Flavorings and Fragrances Using 3D-Printed Catalytic Static Mixers, Ind. Eng. Chem. Res. 60 (2021) 1989-2002. https://doi.org/10.1021/acs.iecr.0c05671

[49] R. Lebl, Y. Zhu, D. Ng, C.H. Hornung, D. Cantillo, C.O. Kappe, Scalable continuous flow hydrogenations using Pd/Al2O3-coated rectangular cross-section 3D-printed static mixers, Catal. Today 383 (2022) 55-63. https://doi.org/10.1016/j.cattod.2020.07.046

[50] J.-N. Tourvieille, R. Philippe, C. de Bellefon, Milli-channel with metal foams under an applied gas–liquid periodic flow: External mass transfer performance and pressure drop, Chem. Eng. J. 267 (2015) 332-346. https://doi.org/10.1016/j.cej.2014.11.084

[51] J.-N. Tourvieille, R. Philippe, C. de Bellefon, Milli-channel with metal foams under an applied gas–liquid periodic flow: Flow patterns, residence time distribution and pulsing properties, Chem. Eng. Sci. 126 (2015) 406-426. https://doi.org/10.1016/j.ces.2014.11.059

[52] R. Munirathinam, J. Huskens, W. Verboom, Supported Catalysis in Continuous-Flow Microreactors, Adv. Synth. Catal. 357 (2015) 1093-1123. https://doi.org/10.1002/adsc.201401081

[53] Ehrfeld Mikrotechnik https://ehrfeld.com/en/products/miprowar.html (accessed 30 November 2021).